

## Resonant magnetic response of TiO<sub>2</sub> microspheres at terahertz frequencies

H. Němec, C. Kadlec, F. Kadlec, P. Kužel, R. Yahiaoui et al.

Citation: *Appl. Phys. Lett.* **100**, 061117 (2012); doi: 10.1063/1.3683540

View online: <http://dx.doi.org/10.1063/1.3683540>

View Table of Contents: <http://apl.aip.org/resource/1/APPLAB/v100/i6>

Published by the [American Institute of Physics](#).

---

### Related Articles

Effect of indium doping on physical properties of nanocrystallized SnS zinc blend thin films grown by chemical bath deposition

*J. Renewable Sustainable Energy* **4**, 011602 (2012)

Enhancement of photoluminescence signal from ultrathin layers with silicon nanocrystals

*Appl. Phys. Lett.* **100**, 061908 (2012)

Nanoassembly control and optical absorption in CdTe-ZnO nanocomposite thin films

*J. Appl. Phys.* **111**, 034305 (2012)

Silver nano particle formation on Ar plasma – treated cinnamyl alcohol

*J. Appl. Phys.* **111**, 034902 (2012)

Enhancement of random lasing assisted by light scattering and resonance energy transfer based on ZnO/SnO nanocomposites

*AIP Advances* **2**, 012133 (2012)

---

### Additional information on *Appl. Phys. Lett.*

Journal Homepage: <http://apl.aip.org/>

Journal Information: [http://apl.aip.org/about/about\\_the\\_journal](http://apl.aip.org/about/about_the_journal)

Top downloads: [http://apl.aip.org/features/most\\_downloaded](http://apl.aip.org/features/most_downloaded)

Information for Authors: <http://apl.aip.org/authors>

## ADVERTISEMENT



**LakeShore Model 8404** developed with **TOYO Corporation**  
**NEW AC/DC Hall Effect System** Measure mobilities down to 0.001 cm<sup>2</sup>/V s

## Resonant magnetic response of TiO<sub>2</sub> microspheres at terahertz frequencies

H. Němec,<sup>1,a)</sup> C. Kadlec,<sup>1</sup> F. Kadlec,<sup>1</sup> P. Kužel,<sup>1</sup> R. Yahiaoui,<sup>2</sup> U.-C. Chung,<sup>3,4</sup> C. Elissalde,<sup>3</sup> M. Maglione,<sup>3</sup> and P. Mounaix<sup>2</sup>

<sup>1</sup>*Institute of Physics, Academy of Sciences of the Czech Republic, Na Slovance 2, 182 21 Prague 8, Czech Republic*

<sup>2</sup>*Laboratoire Ondes et Matière d'Aquitaine (LOMA), Université Bordeaux 1, UMR CNRS 5798, 351 Cours de la Libération, 33405 Talence, France*

<sup>3</sup>*Institut de Chimie de la Matière Condensée de Bordeaux (ICMCB), CNRS—UPR9048, 87 Avenue du Docteur Albert Schweitzer, 33608 Pessac, France*

<sup>4</sup>*Centre de Recherche Paul Pascal—CNRS, Université Bordeaux, 115 Avenue du Dr A. Schweitzer, 33608 Pessac, France*

(Received 2 December 2011; accepted 20 January 2012; published online 9 February 2012)

Spray-drying technique is used to fabricate spherical microparticles out of dissolved TiO<sub>2</sub> nanoparticles. We show both experimentally and through numerical calculations that the microspheres support a Mie resonance, leading to an effective magnetic response. For this purpose, nearly single layers of microspheres were prepared and characterized by time-domain terahertz spectroscopy. We developed an experimental approach allowing simultaneous measurement of complex transmittance and reflectance of a thin layer, which in turn enables evaluation of its effective dielectric permittivity and effective magnetic permeability. Numerical finite-element-method calculations of the electromagnetic response show that the prepared microparticles are suitable for preparing a metamaterial with negative effective magnetic permeability. © 2012 American Institute of Physics. [doi:10.1063/1.3683540]

Electromagnetic metamaterials are artificial structures, which can exhibit specific on-demand optical properties.<sup>1</sup> For example, one can tailor metamaterials with simultaneously negative dielectric permittivity and magnetic permeability,<sup>2</sup> which are of ultimate interest for sub-wavelength imaging applications.<sup>3</sup> While negative permittivity related to the plasma resonance occurs in most metals in a broad spectral range, negative permeability does not naturally occur beyond the gigahertz frequencies.

The dimensions of the metamaterial pattern must be sub-wavelength, which implies micron- or at most tens-micron sized elements for terahertz (THz) metamaterials. Most THz metamaterials reported so far were based on sub-wavelength metallic resonators prepared by lithographical methods.<sup>4</sup> However, negative effective permeability can be also achieved in dielectric resonators in the vicinity of a Mie resonance.<sup>5</sup> A review of Mie resonance-based structures was recently published.<sup>6</sup> Various dielectric metamaterials were proposed, including those with left-handed behavior.<sup>7</sup> However, most of the experimentally tested structures show resonances in the microwave region,<sup>6</sup> while only a few of them were demonstrated in the THz spectral range. For instance, laser micromachining was employed to fabricate a tunable THz metamaterial made of SrTiO<sub>3</sub> rods.<sup>8</sup>

In a vast majority of investigations, only transmission spectra of THz metamaterials are measured, and their agreement with numerical simulations of the metamaterial response is then considered as a proof of their desired properties.<sup>9</sup> In principle, the dielectric and magnetic response can be retrieved when both complex transmittance and complex reflectance spectra are available.<sup>10</sup> In practice, it is difficult

to measure the reflectance phase with high enough accuracy and specific experimental approaches or specific configurations of the time-domain THz spectrometer are needed.<sup>8,11,12</sup>

In this Letter, we report on the resonant response of TiO<sub>2</sub> dielectric microspheres fabricated by a cheap spray-drying technique. We developed an experimental approach allowing measurements of the effective dielectric permittivity and effective magnetic permeability of single-layer films made of such resonators.

Nanoparticles of TiO<sub>2</sub> were mixed with ethanol to obtain a liquid suspension, which was dried upon spraying through flame. This resulted in assembling nanoparticles into fragile mostly spherical clusters. These microspheres were then annealed in a tube furnace at 1200 °C for 2 h, in order to solidify them and to minimize their porosity (Fig. 1(a)). The microspheres were finally sieved and sorted along their diameters  $d$ . We investigated the following powders: (i) MS<sub><38</sub>,  $d < 38 \mu\text{m}$ , (ii) MS<sub>38/40</sub>,  $38 \mu\text{m} < d < 40 \mu\text{m}$ , and (iii) MS<sub>40/50</sub>,  $40 \mu\text{m} < d < 50 \mu\text{m}$ .

We placed a thin layer of TiO<sub>2</sub> microparticles between two thick blocks of sapphire separated by a 70  $\mu\text{m}$  thick Teflon o-ring. This fixes the thickness of the film, which is then essentially composed of a single layer of the microparticles. THz pulses passing through the structure directly carry information about the complex transmittance of the powder, while THz pulses coming from internal reflections in the blocks and from the partial reflection on the sapphire/powder interface carry information also about the complex reflectance of the powder (Fig. 1(b)). These pulses are resolved as a sequence of echoes in the time-domain signal transmitted through the entire structure<sup>13</sup> (see Fig. 1(c)). The sapphire block B is about 2 times thicker than the block A, which ensures that the first internal reflection in the block A does not mix with the internal reflections from the block B. The

<sup>a)</sup>Author to whom correspondence should be addressed. Electronic mail: nemec@fzu.cz.

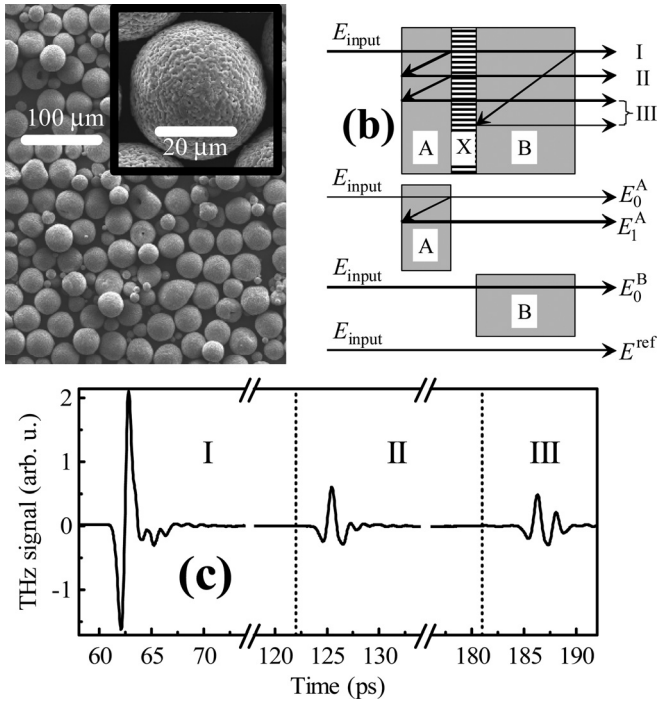


FIG. 1. (a) Scanning electron microscope images of the fabricated TiO<sub>2</sub> microspheres before the sorting procedure. (b) Scheme of the pulse propagation through the structure AXB (sapphire–powder–sapphire) and within the three associated reference measurements. The reflected beams are shifted vertically for graphical clarity. (c) Example of the time-domain signal transmitted through the structure AXB. Dotted lines delimit the intervals containing: I—main pulse ( $E_0^{AXB}$ ); II—1st echo in A ( $E_1^{AXB}$ ); III—superposition of 1st echo in B and 2nd echo in A.

measurement has to be supplemented by three reference measurements: (i) waveform transmitted through the block A (including the first echo), (ii) waveform transmitted through the block B, and (iii) waveform transmitted through an empty space. The complex transmittance and reflectance spectra of the metamaterial are then calculated from

$$t = \frac{E_0^{AXB} E^{\text{ref}}}{E_0^A E_0^B} \cdot \frac{4z_B}{(1+z_A)(1+z_B)}, \quad (1)$$

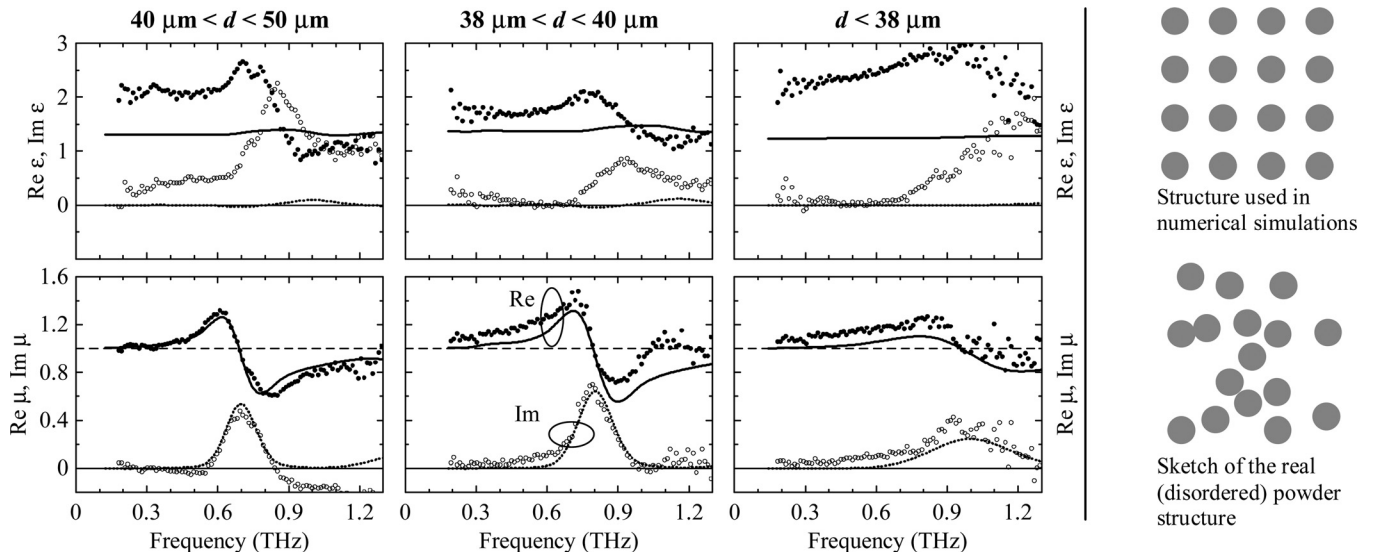


FIG. 2. Permittivity ( $\epsilon$ ) and permeability ( $\mu$ ) of the investigated films. Symbols: measured data; lines: results of numerical simulations with parameters from Table I. Real part: solid line and closed symbols; imaginary part: dotted line and open symbols. Right panel: top—square lattice of TiO<sub>2</sub> microspheres used in numerical simulations; bottom—disordered structure of the powder used in experiments.

$$r = \frac{E_1^{AXB} E_0^A}{E_1^A E_0^{AXB}} \cdot \frac{1 - z_A}{1 + z_A}, \quad (2)$$

where  $z_A$  and  $z_B$  are the relative wave impedances of the blocks A and B, respectively, and  $E$  denotes the Fourier transformations (spectra) of the time-domain signals defined in Fig. 1(b). The use of the same blocks in the reference measurements ensures that the transmittance and reflectance phase is not corrupted by a possible uncertainty in the determination of the thickness of these blocks. We used thick sapphire blocks (3 and 6 mm). The internally reflected pulses (echoes) are thus separated by more than 60 ps (see dotted lines in Fig. 1(c)), which enables a good spectral resolution [ $1/(60 \text{ ps}) \approx 0.03 \text{ THz}$ ]. The effective permittivity and permeability are then retrieved similarly as in Ref. 10.

The experimental results are summarized in Fig. 2. For all three studied powders, we clearly observe the characteristic resonant behavior of the effective magnetic permeability. As expected, the resonance frequency shifts to higher frequencies as the mean particle size decreases. In the static limit, the powder metamaterial should not show any magnetic response.<sup>5</sup> This allows judging the measurement accuracy: at low frequencies, the effective permeability indeed approaches  $1 + 0i$ .

For a deeper insight into the response of the microparticles, we carried out numerical finite-element simulations of a periodic array of microspheres using commercial software Ansoft HFSS. The magnetic resonance is defined by four parameters: the mean size and the permittivity of microspheres mainly determine the resonant frequency, the filling fraction controls the resonance strength, and the polydispersity of particles broadens the resonance.

We assumed that the sieving procedure yields microspheres with well-defined mean diameter for the samples MS<sub>38/40</sub> and MS<sub>40/50</sub> (39 and 45 μm, respectively). Due to the particulate nanostructure of microspheres, their permittivity is isotropic and should be equal to the mean permittivity of rutile ( $\epsilon_T = 114$  (Ref. 14)). Under these conditions, the

simulations give too low resonant frequencies (Fig. 3). However, the nanostructure of the spheres—namely, the presence of air voids within the spheres (Fig. 1(a))—effectively lowers the permittivity of the microspheres themselves; we found that the value of 92 is optimal to match the resonant frequencies. Note that such a difference is not surprising in particulate systems.<sup>15</sup> The mean microsphere diameter for the sample MS<sub><38</sub> is unknown. However, if we assume that the permittivity of these microspheres is also 92, the resonant frequencies are matched for the diameter of 33  $\mu\text{m}$ .

The measured resonance is considerably broader than the resonance observed for the monodisperse microspheres (Fig. 3). This is a consequence of inhomogeneous broadening: the measured permeability spectra can be well matched when a Gaussian distribution of microparticle sizes or refractive indices is considered (Fig. 2 and Table I). These results can be understood as follows. The finest sieve does not limit the smallest particle size, which results in a rather small mean microsphere diameter (33  $\mu\text{m}$ ) and in the broadest distribution of microsphere properties. The smallest spread between particle sizes in MS<sub>38/40</sub> should lead to the narrowest resonance. However, we find that the inhomogeneous broadening is almost the same as that for the MS<sub>40/50</sub>. This indicates that there is a significant distribution in the permittivity of microparticles.

The effective permeability is controlled by the resonances in individual particles, and it is only weakly influenced by the coupling between particles.<sup>8</sup> The corresponding spectra are thus only weakly influenced by the mutual alignment of the microspheres. As a result, there is a good agreement between measured and calculated permeability spectra, despite the fact that a disordered powder was characterized experimentally while a simple square lattice of microspheres was considered in the simulations.

The differences between the measured and calculated permittivity are quite big: simulations provide a lower static permittivity value and no resonance. The low static permit-

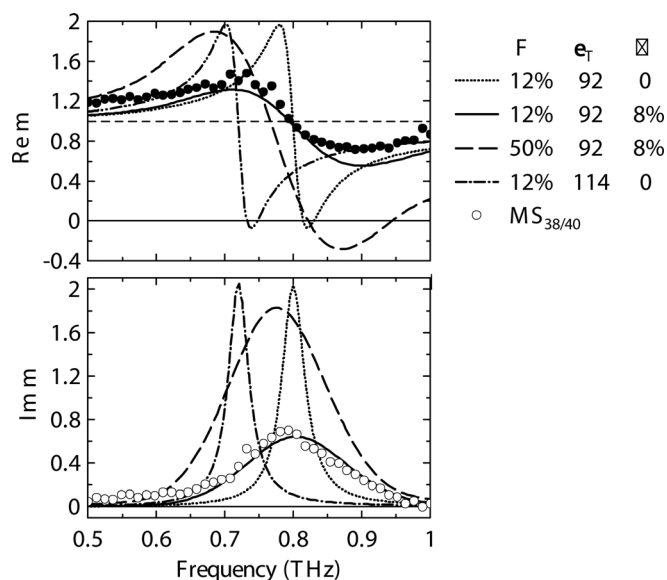


FIG. 3. Lines: calculated permeability of a single layer of monodisperse microspheres with diameter 39  $\mu\text{m}$ .  $F$ : filling factor;  $\epsilon_T$ : permittivity of the microparticles;  $P$ : polydispersity. Symbols: measured permeability of the MS<sub>38/40</sub> sample.

TABLE I. Parameters of the investigated microspheres obtained from the fit of THz permeability spectra; asterisk denotes the nominal microsphere size. Polydispersity stands for the standard deviation of a Gaussian distribution.

Sample	MS <sub>&lt;38</sub>	MS <sub>38/40</sub>	MS <sub>40/50</sub>
Mean diameter ( $\mu\text{m}$ )	33	39*	45*
Polydispersity ( $P$ )	16%	8%	8%
Filling fraction ( $F$ )	8%	12%	10%

tivity is closely related to the low filling factor and low percolation degree, which is controlled by the actual structure of the film.<sup>15</sup> The effective static value obtained from simulations corresponds, as expected, to the Maxwell-Garnet effective medium model with (non-percolated) spherical particles. By contrast, the Lichtenecker effective medium model<sup>16</sup>

$$\epsilon = F\epsilon_T^k + (1 - F) \quad (3)$$

better describes the observed static value ( $\approx 2$ ) for an exponent  $k \approx 0.2$ . This indicates a complex topology of the microspheres network.<sup>16</sup> As an attempt to reproduce the resonant behavior, we performed simulations of the response of the electromagnetic interaction with pairs of microspheres in contact (dimers) arranged in a rectangular lattice. The resonant behavior, similar to the experimental one shown in Fig. 2, then appears in the permittivity spectra for the probing electric field parallel to the dimer axis.

The numerical simulations show that use of much larger filling fraction (e.g., 50%) leads to a metamaterial with slightly negative permeability even in the presence of inhomogeneous broadening (Fig. 3). The investigated microparticles thus may potentially form a negative-permeability metamaterial for large filling fractions, although a narrower distribution would be required to reach, e.g.,  $\mu = -1$ . Unfortunately, the high absorption for filling fractions exceeding  $\sim 15\%$  precluded the experimental permeability determination in such structures.

In summary, spherical TiO<sub>2</sub> microparticles were fabricated by spray-drying technique. A layer of such microspheres exhibits an effective magnetic response related to the presence of Mie resonance. Due to small filling fractions and significant inhomogeneous broadening, negative permeability was not observed, but values considerably lower than 1 are obtained. On the other hand, the numerical simulations showed that negative permeability can be achieved with the investigated microspheres for larger filling fractions.

The financial support by the Grant Agency of ASCR (Project No. A100100907) is acknowledged. The work at the University of Bordeaux 1 was supported by the project ‘‘GIS AMA-SAMM.’’

<sup>1</sup>R. Marqu s, F. Mart n, and M. Sorolla, *Metamaterials with Negative Parameters* (Wiley, NJ, 2008).

<sup>2</sup>R. A. Shelby, D. R. Smith, S. C. Nemat-Nasser, and S. Schultz, *Appl. Phys. Lett.* **78**, 489 (2001).

<sup>3</sup>J. B. Pendry, *Phys. Rev. Lett.* **85**, 3966 (2000).

<sup>4</sup>H.-T. Chen, J. F. O’Hara, A. K. Azad, and A. J. Taylor, *Laser Photon. Rev.* **5**, 513 (2011).

<sup>5</sup>S. O’Brien and J. B. Pendry, *J. Phys.: Condens. Matter* **14**, 4035 (2002).

- <sup>6</sup>Q. Zhao, J. Zhou, F. Zhang, and D. Lippens, *Mater. Today* **12**, 60 (2009).
- <sup>7</sup>K. Vynck, D. Felbacq, E. Centeno, A. I. Cabuz, D. Cassagne, and B. Guizal, *Phys. Rev. Lett.* **102**, 133901 (2009).
- <sup>8</sup>H. Němec, P. Kužel, F. Kadlec, C. Kadlec, R. Yahiaoui, and P. Mounaix, *Phys. Rev. B* **79**, 241108 (2009).
- <sup>9</sup>W. J. Padilla, D. R. Smith, and D. N. Basov, *J. Opt. Soc. Am. B* **23**, 404 (2006).
- <sup>10</sup>D. R. Smith, S. Schultz, P. Markoš, and C. M. Soukoulis, *Phys. Rev. B* **65**, 195104 (2002).
- <sup>11</sup>A. Pashkin, M. Kempa, H. Němec, F. Kadlec, and P. Kužel, *Rev. Sci. Instrum.* **74**, 4711 (2003).
- <sup>12</sup>H. Němec, F. Kadlec, P. Kužel, L. Duvillaret, and J.-L. Coutaz, *Opt. Commun.* **260**, 175 (2006).
- <sup>13</sup>L. Duvillaret, F. Garet, and J.-L. Coutaz, *Appl. Opt.* **38**, 409 (1999).
- <sup>14</sup>R. A. Parker, *Phys. Rev.* **124**, 1719 (1961).
- <sup>15</sup>H. Němec, Z. Mics, M. Kempa, P. Kužel, O. Hayden, Y. Liu, T. Bein, and D. Fattakhova-Rohlfing, *J. Phys. Chem. C* **115**, 6968 (2011).
- <sup>16</sup>A. V. Goncharenko, V. Z. Lozovski, and E. F. Venger, *Opt. Commun.* **174**, 19 (2000).